

COMPARISON OF BERKOVICH AND SPHERICAL TIP INDENTATION FOR DETERMINING THE YOUNG'S MODULUS OF POLYMER THIN FILMS ENCAPSULATED BY A DIELECTRIC

MARINA MELO DE LIMA^{a,b,*}, VINCENT MANDRILLON^b, JENNIFER HAY^c,
LAURENT-LUC CHAPELON^a, CHRISTOPHE POULAIN^b, OLIVIER LEBAGUE^d

^a STMicroelectronics, 850 rue Jean Monnet, 38920 Crolles, France

^b University Grenoble Alpes, CEA-Grenoble, Leti, 17 Avenue des Martyrs, 38054 Grenoble Cedex 9, France

^c KLA Instruments, 105 Meco Lane, Oak Ridge, Tennessee 37830, USA

^d University Grenoble Alpes, CEA-Grenoble, Liten, 17 Avenue des Martyrs, 38054 Grenoble Cedex 9, France

* corresponding author: marina.melodelima@st.com

ABSTRACT.

Pixel integrated micro-lenses for CMOS image sensors consist of a stack of polymer acrylate resin films encapsulated by a dielectric layer. Due to the mismatch of thermomechanical properties, adhesive or cohesive fractures can occur. This can lead to reliability issues requiring the knowledge of the polymer thermomechanical properties. Nanoindentation is a standard method for determining Young's modulus of thin films. However, when performing temperature-dependent nanoindentation studies directly on the polymer film, contamination of the tip can occur near or above the glass transition temperature leading to estimation errors. Therefore, the polymer films must be measured including a protective layer, and a multilayer model is used to extract the polymer's Young's modulus. Finite-element simulations of Berkovich and spherical indentations on the complete stack were performed, enabling the identification of a contact radius range within which the relative error resulting from using the multilayer model is less than 10 %. Consequently, room temperature and temperature-dependent tests of the complete stack were performed, enabling the determination of the polymer's Young's modulus as a function of temperature without tip contamination.

KEYWORDS: Temperature-dependent nanoindentation, Berkovich tip, spherical tip, thin films, polymer, acrylate resin, finite-element modeling.

1. INTRODUCTION

In microelectronics, component manufacturing is based on the triptych of yield, reliability, and performance. This study focuses on the reliability of integrated-pixel micro-lenses for CMOS image sensors. These micro-lenses are composed of a stack of polymer (acrylate) resin films encapsulated by an inorganic and transparent protective layer (Figure 1). The resins that constitute the micro-lenses ensure the convergence of incoming photons onto the underneath photodiodes. The protective layer is a dielectric film added to protect the image sensor during cleaning, packaging, assembly, and from humidity and oxidation throughout the product's lifespan.

One possible limitation of this process is the eventuality of adhesive or cohesive failures due to the mismatch in thermomechanical properties between the protective layer and the polymers.

Consequently, understanding the thermomechanical properties of the polymers is crucial for both identifying the impact of process deposition parameters and providing predictive failure simulations of the complete lens stack. In this study, a polymer provided by STMicroelectronics is characterized to evaluate the evolution of its Young's modulus as a function of

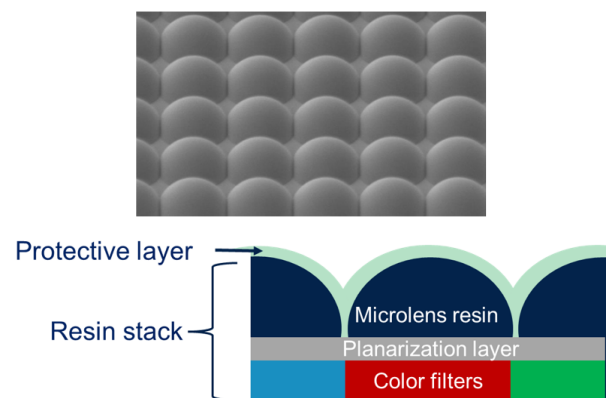


FIGURE 1. SEM image and schematic of a micro-lens array (not to scale).

temperature using temperature-dependent nanoindentation tests.

First, the nanoindentation protocol is described along with the characterized samples. This is followed by the presentation of the analytical multilayer model used to extract the elastic modulus from the experimental data. Then, finite-element models of the indentation are presented and utilized to define

the validity range of the aforementioned analytical model. Afterward, the resulting elastic moduli from room temperature indentations performed with both Berkovich and 50 μm radius spherical tips are compared. Finally temperature-dependent results ranging from 20 to 250 $^{\circ}\text{C}$ are presented. This temperature range is extended up to 250 $^{\circ}\text{C}$ to identify the glass transition temperature.

2. MATERIALS AND METHODS

2.1. EXPERIMENTS

Nanoindentation using a Berkovich tip is the reference method for determining the Young's modulus of thin films. However, when performing temperature-dependent nanoindentation studies directly on a polymer film, contamination of the tip can occur near or above the glass transition temperature leading to estimation errors and tip degradation. Therefore, for the purpose of this study, a dielectric thin film, referred to as the top coat, is added atop the polymer to protect the tip. Consequently, the characterized samples consist of a 3 μm acrylate polymer film deposited on a standard silicon wafer with [100] orientation, encapsulated by a dielectric layer, either 200 nm or 600 nm thick (Figure 2).

However, a potential issue is the cracking of the top coat during indentation, which could lead to tip contamination since it has been demonstrated that room-temperature Berkovich indentation induces such cracks (Figure 2). Therefore, this work focuses first on room-temperature experiments to evaluate and validate the use of a spherical tip, which is less likely to create cracks thanks to its round shape. This is achieved by comparing nanoindentation tests conducted using both Berkovich and 50 μm radius spherical diamond tips. The tested samples include a 3 μm polymer layer deposited on a silicon substrate and two additional samples where the polymer is coated with top coat layers of 200 nm and 600 nm. Temperature-dependent nanoindentation tests, ranging from 20 to 250 $^{\circ}\text{C}$, are then conducted on the complete stack, with a 200 nm thick top coat, using a 50 μm radius sapphire spherical tip. After conducting the test at 250 $^{\circ}\text{C}$, a subsequent test at room temperature is performed for evaluating if the Young's modulus of the polymer comes back to its initial value.

The indentation tests are performed using a MTS XP nanoindenter in Continuous Stiffness Measurement (CSM) mode. This enables real-time contact stiffness measurements and subsequent calculation of the apparent reduced modulus against the contact indentation depth, using the Oliver and Pharr method [1]. The reduced modulus E^* depends on the Young's modulus E and Poisson ratio ν (Eq. 1).

$$E^* = \frac{E}{1 - \nu^2} \quad (1)$$

For the temperature-dependent tests, two independent lasers are used to heat the tip and the backside

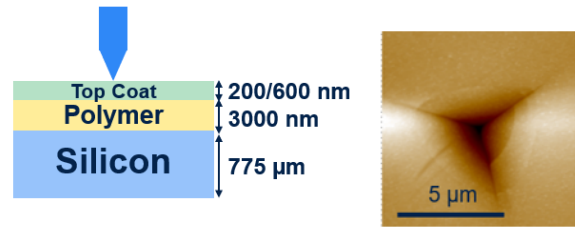


FIGURE 2. Illustration of the stack evaluated during nanoindentation tests (left). AFM image of Berkovich indentation cracks (right).

of the sample *via* optical fibers. The sample is fixed to a specifically-designed stage with a graphite glue allowing heat transfer. The setup also includes a water cooling circuit and a copper shield to protect the indentation column from heating during experiments, which are conducted at ambient air. This system provides a ramping rate of 100 $^{\circ}\text{C min}^{-1}$ and a precise temperature control (± 0.1 $^{\circ}\text{C}$), ensuring that the tip and the sample are at thermal equilibrium before contact. Thermal drift correction is applied by measuring it at 90% of the unloading segment and assuming it remains constant throughout the test. Standard calibration using a fused silica sample is performed before the tests, [1], allowing the use of the tip's real shape for measurement analysis.

2.2. MULTILAYER MODEL

It should be emphasized that the measured reduced elastic modulus is the apparent one of a composite dielectric/resin/substrate modulus. In order to isolate the resin's response, an appropriate bilayer model must be used. Here, the multilayer model of Mercier et al. [2], which extends the monolayer model of Bec et al. [3], is chosen. The Bec model (Eq. 2) involves the reduced modulus of the film and the substrate, respectively E_f^* and E_s^* , the film thickness t and the contact radius r_c . This monolayer model relies on several hypothesis. First that the system's equivalent stiffness can be obtained by applying the reciprocal sum of the film and substrate equivalent stiffnesses. Secondly, that both exhibit elastic behavior. Lastly, that the pressure is applied by a flat cylindrical punch. The relative influences of the film and substrate are weighted by a function derived from finite-element analysis.

$$K_z = \left(1 + \frac{2t}{\pi r_c}\right) \left(\frac{t}{\pi r_c^2 E_f^*} + \frac{1}{2r_c E_s^*}\right)^{-1} \quad (2)$$

The Mercier's multilayer model (Eq. 3) involves the reduced Young's modulus of the layers and the substrate, respectively E_i^* and E_s^* , the films thicknesses t_i , and the calculated contact radius at the layer number i , r_{ci} (Eq. 4).

Properties	Top coat	Polymer	Silicon substrate
Thickness [nm]	200 and 600	3 000	/
Young's modulus [GPa]	42 and 35	[0.1–10]	165 [4]
Poisson ratio	0.23 [5]	0.35 [6]	0.22 [4]

TABLE 1. Material properties used in finite-element simulations. Thicknesses as well as the Young's modulus of the films are experimentally determined. Poisson ratios and the Young's modulus of the substrate are obtained from the literature.

$$K_z = \left(\sum_{i=0}^n \frac{t_i}{(\pi r_{ci}^2 + 2r_{ci}t_i)E_i^*} + \frac{1}{2(r_{cn} + \frac{2t_n}{\pi})E_s^*} \right)^{-1} \quad (3)$$

with

$$r_{c(i+1)} = r_{ci} + \frac{2t_i}{\pi} \quad (4)$$

Here, this multilayer model is used for extracting the Young's modulus of the polymer when encapsulated by a top coat, given that the Young's modulus of the top coat is already known.

3. FINITE-ELEMENT MODEL

The validity of the Mercier's multilayer model depends on several parameters: the mismatch of elastic properties between the films ($E_{topcoat}/E_{polymer}$) and between the films and the substrate ($E_{topcoat}/E_{substrate}$), the contact radius r_c and the ratio of the thicknesses of the films ($t_{topcoat}/t_{polymer}$). Finite-element simulations of the complete stack are conducted to define, for this specific case, the validity domain of the model. The layers' thicknesses, their Young's moduli and Poisson's ratios used in the finite-element simulations are detailed in Table 1. The Poisson's ratio and the Young's modulus of the substrate, suitable to nanoindentation simulations, are obtained from the literature. The Poisson's ratios of the top coat and the polymer are also sourced from literature. The reduced elastic modulus of the 200 nm and 600 nm thick top coat are experimentally determined to be 42 GPa and 35 GPa respectively through nanoindentation tests. The tests are performed at room temperature on a sample consisting of the top coat layer deposited on a silicon substrate. Indentation is carried out using the CSM mode and a standard Berkovich tip. The Bec model is used to extract the Young's modulus. To establish a reference reduced modulus value for the polymer, nanoindentation tests with both Berkovich and 50 μm spherical tip are performed on a 3 μm thick polymer film deposited on a silicon substrate. The reduced elastic moduli obtained from performing 16 indentations on each sample are (4.8 ± 0.3) GPa for the Berkovich tip indentation and (5.5 ± 0.9) GPa for the 50 μm spherical tip indentation.

Here, Berkovich indentation simulations are conducted to study the validity domains of Mercier's multilayer model for room temperature measurements. Therefore, Berkovich indentation simulations are performed by implementing a Young's modulus of 4 GPa,

this value being close to the one measured at room temperature, for the polymer.

Considering that spherical indentation tests are to be performed at elevated temperatures, a consequent reduction in the polymer's Young's modulus is anticipated. Consequently, 50 μm spherical tip indentation simulations are executed across a range of Young's modulus values for the polymer layer, specifically at 0.1, 0.25, 0.5, 1, 2.5, 4, and 10 GPa. Since the elastic properties of the top coat and the substrate are assumed to change little with temperature, they are kept constant and identical to those used for the Berkovich simulations.

3.1. BERKOVICH SIMULATIONS

Finite-element simulations of the indentation of the complete stack are performed with a 70° conical indenter [4], and a tip radius of 20 nm, by assuming an elastic behavior. These axisymmetric, non-linear, two-dimensional simulations are performed using the COSMOS-brand finite-element solver (no longer commercially available).

Both the indenter and the sample are modeled with four-node, axisymmetric, plane-strain elements (Figure 3). For the sample, the extent of the mesh is $90r_c$ in both the radial and axial directions, where r_c , the anticipated contact radius, is calculated as the radius of the indenter at a distance from the apex equal to the specified indentation depth. The radial extent of the fine mesh of the sample is $1.2r_c$. For the indenter, the radial extent of the mesh is $45r_c$, and the axial extent is $90r_c$.

The boundary conditions are specified as follows. Along the right-hand side and bottom of the sample, all nodes are rigidly fixed. Along the axis of symmetry, nodes are constrained to move along the axis of symmetry only ($u_x = 0$). Nodes along the top of the indenter are displaced downward by the total displacement prescribed by the user. Nodes along the right-hand side of the indenter (far from the contact) are unconstrained.

The stiffness of the sample is calculated from the load versus displacement curve by fitting the unloading segment up to 50% of the maximum load. Values of Young's modulus are then calculated, taking into account the indenter's influence [1], and by applying the Sneddon equation [7]. Subsequently, the Mercier's multilayer model is applied to obtain the corrected Young's modulus value for the polymer.

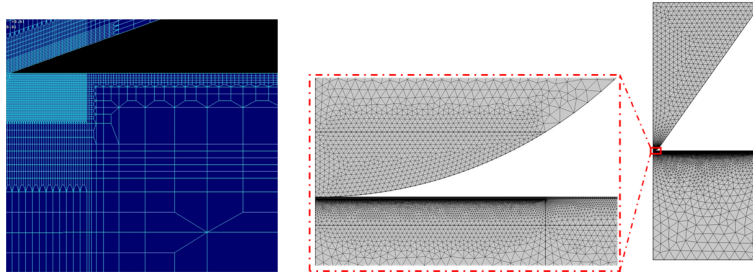


FIGURE 3. Finite element meshes of the tip and films system in the case of a Berkovich (left) and 50 μm spherical (right) indentation.

In this study, simulations are conducted with varying indentation depths to examine the validity of the Mercier’s model depending on the contact radius. Simulations are conducted for top coat thicknesses of both 200 and 600 nm to enable comparison with experimental results.

3.2. SPHERICAL SIMULATIONS

Finite-element simulations are performed with a 50 μm radius spherical tip using the COMSOL software. The tip, the resin thin film and the substrate are modeled with triangular elements, while the top coat is modeled with four-node elements (Figure 3). The mesh for the tip and the sample is refined in the contact area up to $6r_c^{max}$ in both radial and axial directions while the mesh size gradually increases away from the contact region. Regarding boundary conditions, all the nodes are rigidly fixed at the bottom of the sample and a downward displacement, prescribed by the user, is applied to the top of the indenter.

A convergence study validated the built mesh, with relative errors in the Young’s modulus of less than 5% for indentation depths ranging from 2 to 200 nm.

The stiffness of the sample is calculated from the load versus displacement curve by fitting the unloading segment up to 50% of the maximum load. Subsequently, values of reduced Young’s modulus are calculated, accounting for the indenter’s influence [1], and by using the Sneddon [7] equation. Subsequently, the Mercier’s multilayer model is applied to obtain the corrected Young’s modulus value for the polymer.

4. RESULTS AND DISCUSSION

4.1. SIMULATIONS RESULTS

Berkovich and 50 μm spherical indentation simulations, performed with a Young’s modulus of 4 GPa for the polymer, enables the identification of the contact radius range where the Mercier’s multilayer model is valid. The model is considered valid when the relative error in the polymer’s Young’s modulus is below 10%. This range is used to extract an average Young’s modulus value for the polymer from room-temperature nanoindentation tests on the complete stack, in which the polymer is encapsulated by a top coat.

Simulations with a Berkovich tip show that the relative error using the Mercier model remains under 10%

for a contact radius range comprised between 300 and 1400 nm for a capping of 200 nm, and between 600 and 1800 nm for a capping of 600 nm (Figure 4). For the 50 μm spherical tip simulations, with a 200 nm capping, the relative error stays below 10% for a contact radius ranging from 300 to 2750 nm. With a 600 nm capping, the relative error drops below 10% at a contact radius of 1630 nm and stays below 10% up to the maximum studied value of 5100 nm.

These validity ranges are summarized in Table 2 and are used to calculate an average Young’s modulus value from the experimental curves, corrected using the Mercier’s model.

In order to analyze temperature-dependent nanoindentation tests, a second set of indentation simulations is performed with a 50 μm spherical tip and a 200 nm capping, using varying Young’s moduli for the polymer (Figure 4). The results show that the valid contact radius range is dependent on the Young’s modulus of the polymer. Therefore, to analyze the temperature-dependent tests, an average Young’s modulus is calculated using a common contact radius range. This range corresponds to 1600–2500 nm. However, for the specific case of a polymer with a Young’s modulus of 0.1 GPa, the relative error remains between 12% and 16% and since a Young’s modulus value of 0.1 GPa is expected only above the glass transition temperature, this error margin is considered reasonable. Therefore an average Young’s modulus for the polymer will be extracted within this range for all temperature studied, with the understanding that values obtained above the glass transition temperature may be less confident.

4.2. EXPERIMENTAL RESULTS AT ROOM TEMPERATURE

Experimental curves obtained at room temperature by indenting the following stack: 200 nm top coat/3 μm polymer/silicon substrate, are shown in Figure 5. The black and gray lines represent indentation performed with a Berkovich tip and a 50 μm spherical tip, respectively. The dashed lines indicate the apparent Young’s modulus while the solid lines show the corrected Young’s modulus using the Mercier’s model. An average Young’s modulus value is calculated within the contact radius range determined from the simu-

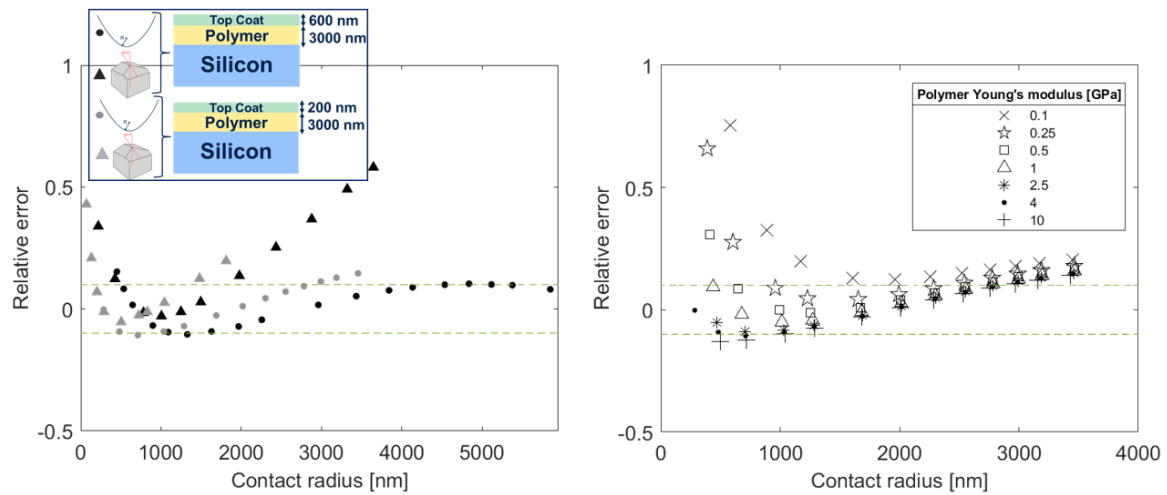


FIGURE 4. Relative error in the Young's modulus of the polymer, using the Mercier's model, according to finite-element simulations indentations on the stack: top coat/polymer/silicon. Simulations were conducted for varying top coat thicknesses (left graph). In this graph, gray indicates Berkovich simulations, while black denotes 50 μm spherical indentations. Circles and triangles represent cases of the polymer encapsulated by top coats of 600 nm and 200 nm thickness, respectively. The right graph displays results from 50 μm spherical indentation simulations for different Young's moduli of the polymer.

Stack	Valid r_c and h ranges [nm]	
	Berkovich tip	50 μm spherical tip
Top coat (42 GPa - 200 nm)/Polymer (4 GPa - 3 μm)/Silicon	200-400/150-650	300-2750/2-130
Top coat (35 GPa - 600 nm)/Polymer (4 GPa - 3 μm)/Silicon	600-1800/350-920	500-5100/7-600
Top coat (42 GPa - 200 nm)/Polymer (0.1-10 GPa - 3 μm)/Silicon	/	1 600-2 500/50-110

TABLE 2. Valid contact radius (r_c) and indenter displacement (h) ranges, extracted from the simulation results, depending on the stack under study and the indentation tip.

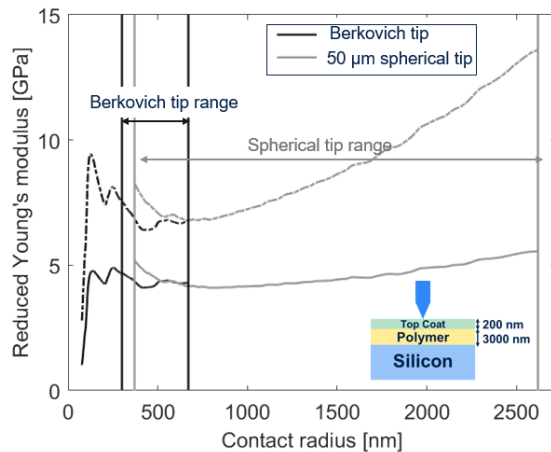


FIGURE 5. Evolution of the Young's modulus as a function of the contact radius (derived from calibration data) for an indented stack consisting of 200 nm top coat/3 μm polymer/silicon substrate. The dashed lines represent the apparent Young's modulus and the solid lines the Young's modulus corrected using the Mercier's model. Indentations were performed with Berkovich (black curves) and 50 μm spherical (gray curves) tips. The vertical lines show the contact radius range used for extracting an average Young's modulus value.

lations and using the Mercier-corrected curve. This range is delineated by the black and gray vertical lines for the Berkovich and 50 μm spherical indentations, respectively. These results enable the acquisition of the Young's modulus of the polymer encapsulated with a 200 nm capping (Figure 6). The same protocol is used for a capping of 600 nm.

Coherent values for the Young's modulus of the polymer (Figure 6) are obtained, with a minimum of 4.3 GPa and a maximum of 5.5 GPa. It enables the validation of this protocol at room temperature.

4.3. TEMPERATURE DEPENDENT EXPERIMENTAL RESULTS

The obtained reduced Young's modulus of the polymer on a silicon substrate encapsulated by a 200 nm top coat as a function of temperature is shown in Figure 6. Here, the protocol used allows obtaining the value of the reduced Young's modulus above the glass transition temperature, without tip contamination. Tests performed at room temperature after heating at 250 $^{\circ}\text{C}$ show that the polymer recovers its initial reduced Young's modulus. This demonstrates that the polymer was sufficiently stabilized through thermal annealing before conducting the temperature-dependent nanoindentation test. The glass transition temperature is determined to be around 220 $^{\circ}\text{C}$ by

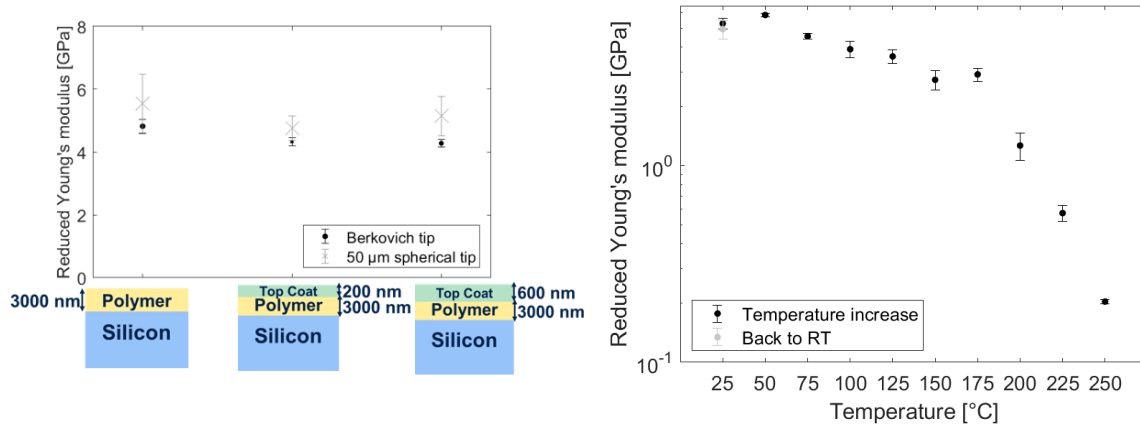


FIGURE 6. Average Young's modulus values determined for different samples, at room temperature, using Berkovich and 50 μm spherical tips (right graph). Average Young's modulus of the polymer as a function of temperature (left graph). The polymer film is deposited on a silicon substrate and encapsulated by a 200 nm top coat. Tests were performed with a 50 μm spherical tip.

identifying the inflection point on the curve. This value is consistent with previous studies conducted by temperature-dependent wafer curvature tests and presented as the results for 'resin C' in [8].

5. CONCLUSIONS

A protocol for temperature-dependent nanoindentation of polymer thin films without tip contamination is described and validated. It involves adding a top coat, here a dielectric capping, and the use of the Mercier's multilayer model to extract the Young's modulus of the polymer. The applicability of this model to the stack studied here is verified by finite-element simulations of Berkovich and 50 μm spherical tip indentations. This enabled the identification of a contact radius range for which the relative error in Young's modulus is less than 10%. Consequently, the evolution of the Young's modulus of the polymer as a function of temperature is determined while preventing tip contamination.

ACKNOWLEDGEMENTS

This work is part of the IPCEI Microelectronics and Connectivity and was supported by the French Public Authorities with the frame of "France 2030" program.

REFERENCES

- [1] W. C. Oliver, G. M. Pharr. An improved technique for determining hardness and elastic modulus using load and displacement sensing indentation experiments. *Journal of Materials Research* **7**(6):1564–1583, 1992. <https://doi.org/10.1557/JMR.1992.1564>
- [2] D. Mercier, V. Mandrillon, M. Verdier, Y. Brechet. Mesure de module d'Young d'un film mince à partir de

mesures expérimentales de nanoindentation réalisées sur des systèmes multicouches. *Matériaux & Techniques* **99**(2):169–178, 2011.

<https://doi.org/10.1051/mattech/2011029>

- [3] S. Bec, A. Tonck, J. L. Loubet. A simple guide to determine elastic properties of films on substrate from nanoindentation experiments. *Philosophical Magazine* **86**(33-35):5347–5358, 2006. <https://doi.org/10.1080/14786430600660856>
- [4] M. Rusinowicz. *Mechanical and electrical properties of dielectric thin films: electrical-nanoindentation experiments and numerical simulations*. Ph.d. thesis, Université Grenoble Alpes, 2023.
- [5] G. Carlotti, N. Chérault, N. Casanova, et al. Elastic constants of low- k and barrier dielectric films measured by Brillouin light scattering. *Thin Solid Films* **493**(1-2):175–178, 2005. <https://doi.org/10.1016/j.tsf.2005.06.019>
- [6] J. Richeton, S. Ahzi, K. Vecchio, et al. Modeling and validation of the large deformation inelastic response of amorphous polymers over a wide range of temperatures and strain rates. *International Journal of Solids and Structures* **44**(24):7938–7954, 2007. <https://doi.org/10.1016/j.ijsolstr.2007.05.018>
- [7] I. N. Sneddon. The relation between load and penetration in the axisymmetric Boussinesq problem for a punch of arbitrary profile. *International Journal of Engineering Science* **3**(1):47–57, 1965. [https://doi.org/10.1016/0020-7225\(65\)90019-4](https://doi.org/10.1016/0020-7225(65)90019-4)
- [8] B. Vavrille. *Développement d'une méthode innovante de mesures des propriétés thermomécaniques de films minces. Application à un dispositif imageur*. Ph.d. thesis, Université Grenoble Alpes, 2023.